Inorg. Chem. **2005**, *44*, 7394–7402

Tribasic Lead Maleate and Lead Maleate: Synthesis and Structural and Spectroscopic Characterizations

François Bonhomme,[†] Todd M. Alam,[‡] Aaron J. Celestian,[⊥] David R. Tallant,[§] Timothy J. Boyle,[||] Brian R. Cherry,[‡,#] Ralph G. Tissot,[*,§] Mark A. Rodriguez,[§] John B. Parise,[⊥] and May Nyman[†]

Geochemistry Department, Sandia National Laboratories, Albuquerque, New Mexico 87185-0754, Department of Biomolecular and Chemical Analysis, Sandia National Laboratories, Albuquerque, New Mexico 87185-0886, Materials Characterization Department, Sandia National Laboratories, Albuquerque, New Mexico 87185-1411, Inorganic Chemistry and Nanomaterials, Advanced Materials Laboratory, Sandia National Laboratories, 1001 University Boulevard SE, Albuquerque, New Mexico 87106, and Center for Environmental and Molecular Sciences, Stony Brook University, Stony Brook, New York 11794-2100

Received April 20, 2005

We report on the synthesis and structure of tribasic lead maleate hemihydrate ($[Pb_4O_3]C_2H_2(CO_2)_2 \cdot {}^1/_2H_2O$, TRIMAL) and lead maleate ($PbC_2H_2(CO_2)_2$, PBMAL). The structure of $[Pb_4O_3]C_2H_2(CO_2)_2 \cdot {}^1/_2H_2O$, solved ab initio from X-ray powder diffraction data, consists of infinite slabs of edge-sharing OPb_4 tetrahedra, of composition $[Pb_4O_3]$, running along the *c* axis and linked together into a three-dimensional network by tetradentate maleate anionic ligands. The structure of $PbC_2H_2(CO_2)_2$, solved from single crystal diffraction data, is lamellar and contains double layers of heptacoordinated lead atoms, bonded only to the oxygen atoms of the maleate ligands. In both compounds, lead is in the oxidation state 2+ and the coordination polyhedra around the Pb^{2+} exhibit a hemidirected geometry and are strongly distorted as a result of the lone pair of electrons. The absence of protons on the acidic portion of the maleate moieties was confirmed by Raman spectroscopy and by ^1H MAS and ^1H–^{13}C CP MAS NMR experiments. The two compounds were further characterized using chemical and thermogravimetric analyses.

Introduction

Basic lead carboxylates are extremely active heat stabilizers for halogenated polymers such as poly(vinyl chloride) and act as scavengers for the HCl evolved during the alteration of the polymer, thereby slowing down its degradation. In these phases, the lead atoms are bonded to both polydentate-deprotonated carboxylate moieties and to oxygen atoms that do not belong to these ligands. Mono-, di-, tri-, and tetrabasic compounds are known, and this commonly used nomenclature describes the number of formal (PbO) units in their empirical formulas. Their performance at stabilizing poly(vinyl chloride) is comparable to that of the state-of-the-art organotin mercaptide compounds.[1] These lead phases, based on their assigned empirical formulas, are simply described as small insoluble filler pieces of litharge to which various organic groups are attached to improve molecular level mixing with the polymer matrix. Tribasic lead maleate (given in the literature as $3(PbO) \cdot PbC_2H_2(CO_2)_2 \cdot {}^1/_2H_2O$, hereafter TRIMAL) is one of several basic lead carboxylates used as a heat stabilizer for halogenated polymers.[1,2] The mechanisms by which these phases function as stabilizers and modifiers are not fully understood. Therefore, the knowledge of the structural details of these industrially important phases is pertinent to understanding the reactions responsible for their heat-stabilizing properties and to guiding the development of optimized lead-based additives.

To our knowledge, however, no basic lead carboxylate phase commercially used as a stabilizer has yet been structurally characterized. These compounds are extremely

* To whom correspondence should be addressed. E-mail: rgtisso@sandia.gov. Fax: (505) 844-9781.
[†] Geochemistry Department, Sandia National Laboratories.
[‡] Department of Biomolecular and Chemical Analysis, Sandia National Laboratories.
[§] Materials Characterization Department, Sandia National Laboratories.
[||] Inorganic Chemistry and Nanomaterials, Advanced Materials Laboratory, Sandia National Laboratories.
[⊥] Stony Brook University.
[#] Present address: Bruker Biospin Inc., Billerica, MA.

(1) Grossman, R. F.; Krausnick, D. *J. Vinyl Addit. Technol.* **1997**, *3*, 7.
(2) Grossman, R. F. *J. Vinyl Addit. Technol.* **1999**, *5*, 148.

10.1021/ic050611y CCC: $30.25
Published on Web 09/10/2005

insoluble in their synthesis media and so far obtaining crystals suitable for single-crystal X-ray diffraction has not been realized. Previously, a series of basic lead stabilizers had been studied by NMR and IR spectroscopies;[1,2] however, no definitive structural information was forthcoming.

We report here the structure determination of TRIMAL from X-ray powder diffraction data, ^{1}H magic angle spinning (MAS) and ^{1}H−^{13}C cross-polarized (CP) MAS NMR, and Raman spectroscopy. To establish a baseline for the interpretation of the TRIMAL data, we also synthesized and characterized in parallel a related coordination compound, lead maleate ($PbC_2H_2(CO_2)_2$, PBMAL), for which a single-crystal X-ray structure was solved.

Experimental Section

Synthesis. All of the following starting materials were used as received: acetic acid (Aldrich), maleic anhydride (Aldrich), maleic acid (Fisher), and litharge/massicot (PbO; Baker Chemical Co.).

(a) $[Pb_4O_3]C_2H_2(CO_2)_2 \cdot {}^1/_2H_2O$ (TRIMAL). The following preparation was undertaken based on minor modifications to the manufacturing specifications supplied by Halstab, a Division of Hammond Group, Inc., Hammond, IN. The synthesis was carried out using standard Schlenk line techniques. PbO (10.80 g, 48.3 mmol) was slurried in 250 mL of deionized (DI) water. To the stirring mixture was added via syringe acetic acid (0.20 g, 3.33 mmol). The reaction was warmed to about 50 °C, and maleic anhydride (6.00 g, 61.2 mmol) was slowly added via syringe. After the reaction mixture was stirred for about 4 h, the volatile portion was removed by vacuum distillation. After drying, the powder was washed repeatedly with water and used without further purification. A quantitative conversion of the PbO precursor to TRIMAL was recorded.

(b) $PbC_2H_2(CO_2)_2$ (PBMAL). PbO (5.00 g, 22.4 mmol) was mixed in 300 mL of DI water; maleic acid (2.60 g, 22.4 mmol) was dissolved at 25 °C in 100 mL of DI water, and the resulting solution was added under agitation to the PbO/water mixture. The reaction mixture was then heated in an open beaker to 70 °C and stirred continuously for 2 h. After cooling to room temperature, an off-white crystalline powder was recovered by filtration, washed repeatedly with water, and dried in air overnight at room temperature. The overall yield of the reaction is 85% (6.21 g of product recovered).

Characterization. X-ray powder diffraction was performed with a Bruker D8 Advance diffractometer in Bragg−Brentano geometry with Ni-filtered Cu Kα radiation. Single-crystal diffraction data for PBMAL were collected at room temperature using a Bruker AXS P4 diffractometer equipped with a SMART 1000 CCD camera, with Mo Kα radiation.

The solid-state ^{1}H MAS NMR spectra were measured on a Bruker Avance 600 operating at a proton frequency of 600.1 MHz using a 2.5-mm broad-band double-resonance probe spinning at 30 kHz. The ^{1}H chemical shift is referenced to the secondary standard adamantane ($\delta = 1.63$) with respect to tetramethylsilane (TMS; $\delta = 0.0$). The solid-state ^{13}C CP MAS NMR spectra were obtained on a Bruker Avance 400 operating at a carbon frequency of 100.63 MHz using a 4-mm broad-band double-resonance probe spinning at 10 kHz. A variable-amplitude cross-polarization sequence with a 3-μs ^{1}H $\pi/2$ pulse, a 2-ms contact pulse, 1024 scan averages, a 10-s recycle delay, and a two-pulse phase-modulated ^{1}H decoupling was utilized. The ^{13}C NMR chemical shifts were referenced to the secondary standard of the carbonyl resonance of glycine ($\delta = 176$), with respect to TMS ($\delta = 0$). The solid-state double-quantum (DQ) correlation experiments utilized the offset-compensated back-to-back multiple-pulse train for the excitation and reconversion of multiple-quantum coherences. The sequence used a 64-step phase cycle, with 128 rotor-synchronized t_1 increments, and a excitation/reconversion length of 133 μs ($4\tau_R$), with States-TPPI (time proportional phase increment) phase detection in the F_1 dimension.

Raman spectra were obtained using for excitation the 514-nm line of an Ar laser operating at 1 mW. A microscope accessory with a magnification of 80×, a triple spectrograph, and a charge-coupled-device detector were used to collect the spectra. Samples were examined with a JEOL 6300V scanning electron microscope. Thermal analysis was performed with a TA Instruments SDT Q600 simultaneous TGA-DSC under an argon or air flow of 100 cm^3/min with a heating rate of 5 °C/min. Lead elemental analysis was executed on a Perkin-Elmer Sciex Elan 6100 ICP-MS using an argon plasma flame, with the samples having been dissolved in hot nitric acid. The carbon and hydrogen contents were determined by the combustion method using a Leco CHN-900 analyzer. The sample density was determined using a Micromeritics AccuPyc 1330 helium displacement pycnometer.

Structure Determination. The structure of TRIMAL was solved ab initio from powder diffraction data. The small size of the blade-shaped crystallites (less than 700 nm, with an aspect ratio of larger than 10, as determined from scanning electron microscopy micrographs) led to significant peak broadening, with the minimum full width at half-maximum (fwhm) being 0.16°, about 3 times the instrumental resolution. The powder pattern was indexed by the program TREOR90[3] with a monoclinic *C*-centered cell of approximately 1021 Å^3. The refined lattice constants are given in Table 1. The extinction laws are consistent with the space group *C*2/*c* and, of course, *Cc*. A whole pattern profile refinement by the Le Bail method[4] (program FULLPROF2K[5]) with the space group *C*2/*c* converged to $\chi^2 = 7.27$ and confirmed the adequacy of this cell and systematic absences. The structure was solved in *C*2/*c* using the direct-space reverse Monte Carlo optimization method as implemented in the program FOX[6] coupled with manual model buildup. No structure solution was found using the space group *C*2/*m* or *Cm*, which are also allowed by the extinction laws. The chemical analyses and observed density indicated that 16 lead atoms were present per unit cell. The coordinates of two independent lead sites in general positions were immediately revealed. The wide variability generally observed of the oxygen coordination of Pb^{2+} precluded the use of regular polyhedral building units in the optimization process and complicated further the completion of the structure.[7] At that stage, difference Fourier synthesis did not reveal any chemically sensible site. However, the examination of the Pb−Pb distances allowed us to determine the likely position of three oxygen sites tetrahedrally bonded only to lead, with bond distances ranging from 2.3 to 2.7 Å. A Rietveld refinement of this partial model confirmed its validity and allowed us to proceed with the location of the organic acid. We kept fixed these two lead and three oxygen sites previously found, introduced a maleic acid molecule in the model, and optimized its position and orientation with FOX. This so-obtained model was then fully refined by the

(3) Werner, P. E.; Eriksson L.; Westdahl, M. *J. Appl. Crystallogr.* **1985**, *18*, 367.
(4) Le Bail, A.; Duroy H.; Fourquet, J. *Mater. Res. Bull.* **1988**, *23*, 447.
(5) Rodriguez-Carvajal, J. A. *Collected Abstracts of Powder Diffraction Meeting*, Toulouse, France, 1990; p 127.
(6) Favre-Nicolin, V.; Cerny, R. *J. Appl. Crystallogr.* **2002**, *35*, 734.
(7) Shimoni-Livny, L.; Glusker, J. P.; Bock, C. W. *Inorg. Chem.* **1998**, *37*, 1853.

Table 1. Crystal Data and Structure Refinement Parameters for TRIMAL

compound	$[Pb_4O_3]C_2H_2(CO_2)_2 \cdot {}^1/_2H_2O$
formula weight	999.8 g
crystal system	monoclinic
space group	*C*2/*c*
unit cell dimensions	$a = 11.3720(9)$ Å
	$b = 17.272(1)$ Å
	$c = 5.7028(4)$ Å
	$\beta = 114.250(4)°$
volume	1021.3(1) Å^3
Z	4
density (calcd, obsd)	6.50, 6.69(4) g/cm^3
temperature	298(2) K
wavelength	Cu Kα
2θ range	8.0−80.0°
step size 2θ	0.04°
time per step	40 s
min fwhm	0.16°
no. of independent atoms	10
no. of refined param[a]	63
no. of structural param[a]	23
no. of "independent" reflections	426
final *R* indices	$R_p = 6.21\%$; $R_{wp} = 8.37\%$
	$R_{exp} = 2.20\%$; $\chi^2 = 14.4$
	$R_{Bragg} = 3.23\%$
soft constraints	C=C = 1.33(1) Å; C−C = 1.47(1) Å
	C−O = 1.25(2) Å; C=C−C = 130(1)°
	C−C−O = 120(1)°; O−C−O = 120(1)°
	C−C=C−C = 0(1)°

[a] 21 positional parameters and 2 isotropic atomic displacement parameters; 13 profile parameters and 27 linearly interpolated background points.

Table 2. Selected Interatomic Distances for TRIMAL

Pb1−O3	2.24(4)	Pb2−O4	2.26(5)
Pb1−O5	2.25(1)	Pb2−O5	2.39(2)
Pb1−O4	2.34(5)	Pb2−O1	2.43(4)
Pb1−O3	2.37(5)	Pb2−O2	2.48(4)
Pb1−O1	3.18(3)	Pb2−O2	3.15(4)
Pb1−O1	3.27(4)	Pb2−O2	3.17(4)
Pb1−Ow	2.30 average	Pb2−O2	3.21(5)

Rietveld method, using bond distance and angle restraints for the maleate moiety, corresponding to the geometric values found in the literature.[8,9] The refinement eventually converged to a satisfactory agreement factor $R_{Bragg} = 3.29\%$ and $\chi^2 = 14.78$. With the help of the ^{1}H MAS NMR analysis, a reasonable position for a water molecule with 25% occupancy was determined and its inclusion in the model improved the agreement factors to $R_{Bragg} = 3.22\%$ and $\chi^2 = 14.42$. The relatively high χ^2 is due to difficulties in modeling the peak profiles, which are slightly affected by anisotropic peak broadening because of the anisotropic size of the crystallites. The Le Bail fit, where the profile intensities are not constrained by a structural model, did converge only down to $\chi^2 = 7.27$, confirming that the high residuals are mostly due to an inadequate profile description. Attempts to model an *hkl*-dependent peak width failed, likely because many extra profile parameters are necessary with a crystal structure of low symmetry. A summary of crystallographic data, including the values of the geometrical constraints and measurement conditions, is given in Table 1. Selected interatomic distances are given in Table 2. A CIF file containing the atomic coordinates is deposited as Supporting Information. The observed, calculated, and difference Rietveld plots are given in Figure 1.

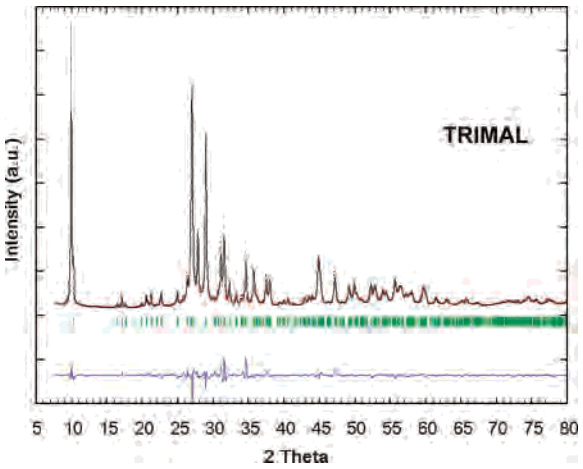

Figure 1. Observed (red dots), calculated (black line), and difference (blue line) Rietveld patterns for TRIMAL.

Table 3. Crystal Data and Structure Refinement for PBMAL

compound	$Pb[C_2H_2(CO_2)_2]$
formula weight	321.2 g
crystal system	monoclinic
space group	$P2_1/c$
unit cell dimensions	$a = 9.920(3)$ Å
	$b = 6.9793(18)$ Å
	$c = 8.293(2)$ Å
	$\beta = 111.094(6)°$
volume	535.7(2) Å^3
Z	4
density (calcd, obsd)	3.98, 3.96(2) g/cm^3
temperature	293(2) K
wavelength	0.71073 Å
absorption coefficient	31.4 mm^{-1}
F(000)	560
crystal size	0.050 × 0.030 × 0.009 mm
θ range for data collection	2.20−8.23°
index ranges	$-12 \le h \le 12$, $-8 \le k \le 8$,
	$-10 \le l \le 10$
reflections collected	3739
independent reflections	1242 [R(int) = 0.0530]
completeness to $\theta = 28.23°$	93.9%
refinement method	full-matrix least-squares on F^2
data/restraints/parameters	1242/0/83
goodness of fit on F^2	1.038
final *R* indices [$I > 2\sigma(I)$]	R1 = 0.0338, wR2 = 0.0785
R indices (all data)	R1 = 0.0428, wR2 = 0.0853
extinction coefficient	0.0040(5)
largest diff. peak and hole	2.437 and −1.703 e Å^{-3}

The crystal structure of PBMAL was solved from single-crystal data by direct methods (program SIR97[10]), completed by difference Fourier syntheses, and refined by full matrix least squares (program SHELXL97[11]). All non-hydrogen atoms were refined anisotropically; the hydrogen atoms were placed geometrically and refined using the riding atom model. A summary of crystallographic data is given in Table 3, selected interatomic distances are given in Table 4, and a CIF file is deposited as Supporting Information. All of the peaks present in the powder diffraction pattern of PBMAL could be indexed by the single-crystal unit cell, thereby confirming the absence of crystalline impurities in the bulk sample.

(8) Cernak, J.; Chomic, J.; Kappenstein, C.; Robert, F. *J. Chem. Soc., Dalton Trans.* **1997**, 2981.
(9) James, M. N. G.; Williams, G. J. B. *Acta Crystallogr.* **1974**, *B30*, 1249.
(10) Altomare, A.; Burla, M. C.; Camalli, M.; Cascarano, G. L.; Giacovazzo, C.; Guagliardi, A.; Moliterni, A. G. G.; Polidori, G.; Spagna, R. *J. Appl. Crystallogr.* **1999**, *32*, 115.
(11) Sheldrick, G. M. *Programs for Crystal Structure Analysis* (Release 97-2); Institüt für Anorganische Chemie der Universität: Göttingen, Germany, 1998.

Table 4. Selected Interatomic Distances for PBMAL

Pb−O4	2.423(6)	Pb−O4	2.688(6)
Pb−O1	2.453(6)	Pb−O1	2.741(7)
Pb−O2	2.524(7)	Pb−O3	2.860(8)
Pb−O3	2.619(7)		
O4−C4	1.286(11)	O2−C4	1.254(11)
O3−C1	1.243(12)	O1−C1	1.282(11)
C3−C2	1.342(14)	C2−C1	1.496(14)
C4−C3	1.462(13)		
C2−H2	0.93	C3−H3	0.93

Results and Discussion

Synthesis. The synthesis of both of these maleate lead compounds use maleic acid to complex and dissolve the PbO precursor; however, TRIMAL uses a maleic anhydride/Pb ratio of 1.27:1 with a catalytic amount of acetic acid (~5% of the anhydride concentration). This reaction is designed for slow conversion of the maleic anhydride to maleic acid by the weak acetic acid. PBMAL, on the other hand, is synthesized under more harsh conditions using a 1:1 mixture of PbO/maleic acid, which results in a faster digestion of PbO. This is easily observed by the rapid change of the original yellow-orange slurry of litharge in water to creamy off-white upon the addition of maleic acid for PBMAL in comparison to the slow change observed for TRIMAL.

These different reaction conditions led to different types of structures (see below). TRIMAL is essentially a network of infinite Pb−O slabs, related to those found in the litharge precursor, that are linked together by maleate ligands. On the other hand, PBMAL is composed of polymeric lead/maleate coordination complexes, and all of the oxygens bonded to the lead originate from the maleate species.

Structure Description. For TRIMAL, the lone pair of electrons on the two independent Pb^{2+} atoms causes their coordination geometry to be distorted and hemidirected.[7] There are two groups of Pb−O distances present in the structure, one ranging from 2.24(4) to 2.48(4) Å and the other from 3.15(4) to 3.27(4) Å. Using 3.30 Å as the cutoff, the Pb1 and Pb2 coordination numbers are six and seven, respectively. Each lead atom has four short Pb−O bonds and two or three long Pb−O bonds. The structural environments of the lead atoms and Pb−O distances are shown in Figure 2, with the lone pair approximately directed opposite to the short Pb−O bonds. The discussion of the extended structure based on the linkage of these PbO_6 and PbO_7 distorted polyhedra would be quite complex however. The crystal structure is better understood by considering the coordination polyhedra of some of the oxygen atoms.[12] The three independent oxygen atoms that do not belong to the maleate ligand (O3, O4, and O5) are tetrahedrally coordinated by lead atoms, with Pb−O distances ranging from 2.24(4) to 2.39(2) Å. The average Pb−O and Pb−Pb distances for these three independent tetrahedra are 2.31 and 3.76 Å, respectively, and correspond closely to the values observed in litharge[13] (2.31 and 3.77 Å). The three independent OPb_4 tetrahedra share edges with each other and

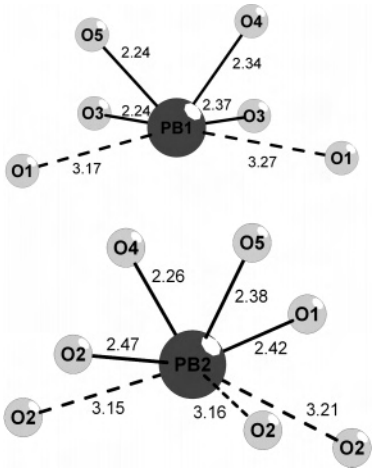

Figure 2. Coordination and Pb−O distances (Å) around Pb1 and Pb2 in TRIMAL.

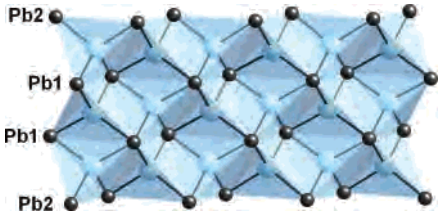

Figure 3. Infinite $[Pb_4O_3]$ slab in TRIMAL, built up by (OPb_4) tetrahedra, viewed approximately along the *a* axis (lead, small black spheres; oxygen, big blue spheres).

form infinite slabs running along *c*, with a height of three tetrahedra along *b* and a thickness of one tetrahedron along *a* (see Figure 3), giving a composition of $[Pb_4O_3]$. The translation period of the $[Pb_4O_3]$ slab is 5.70 Å (i.e., the *c* cell parameter of TRIMAL), which is similar to 5.71 and 5.81 Å observed for the related $[Pb_3O_2]$ slabs found in lead oxide hydroxide nitrate phases.[14,15] Pb2 belongs to the peripheral tetrahedra and is located on the top and bottom of the slabs, whereas Pb1 occupies the middle section. Each tetradentate ligand is bonded to three adjacent slabs through four O−Pb2 bonds of 2.43(4) and 2.48(4) Å and link these slabs together in the *ab* plane, thereby forming a three-dimensional structure. These Pb−O distances are similar to those encountered in lead diphosphonate,[16] for example. Each $[Pb_4O_3]$ slab is thus bonded to six neighboring slabs (see Figure 4). The anisotropy of the structure is reflected in the morphology of the crystallites, which are thin elongated plates. Each oxygen atom of the maleate makes only one bond with a lead atom, Pb2 (see Figure 5). Although many lead compounds containing related infinite slabs built up by edge-sharing oxo-centered OPb_4 tetrahedra are known, especially with slab compositions $[Pb_2O]$ or $[Pb_3O_2]$,[12] this is to our knowledge the first observation of a $[Pb_4O_3]$ unit.

PBMAL adopts a two-dimensional (2D) structure wherein lead maleate double layers are arranged parallel to the *bc*

(12) Krivovichev, S. V.; Armbruster, T.; Depmeier, W. *J. Solid State Chem.* **2004**, *177*, 1321.
(13) Boher, P.; Garnier, P.; Gavarri, J. R.; Hewat, A. W. *J. Solid State Chem.* **1985**, *57*, 343.
(14) Li, Y.; Krivovichev, S. V.; Burns, P. C. *J. Solid State Chem.* **2000**, *153*, 365.
(15) Krivovichev, S. V.; Li, Y.; Burns, P. C. *J. Solid State Chem.* **2001**, *158*, 78.
(16) Irran, E.; Bein, T.; Stock, N. *J. Solid State Chem.* **2003**, *173*, 293.

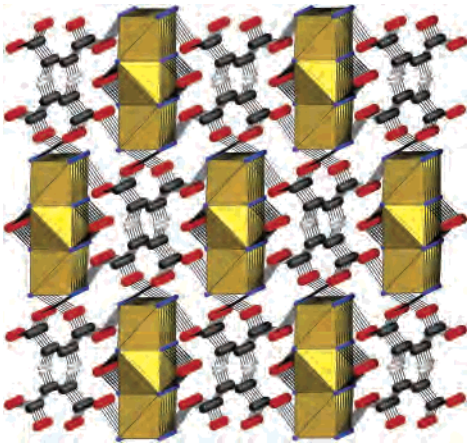

Figure 4. View of TRIMAL, approximately along the *c* axis (yellow, OPb_4 tetrahedra; black spheres, carbon; red spheres, oxygen; white spheres, hydrogen; blue spheres, lead).

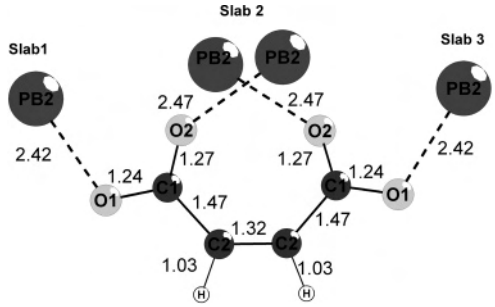

Figure 5. Tetradentate maleate ligand linking three slabs together and relevant distances (Å) in TRIMAL.

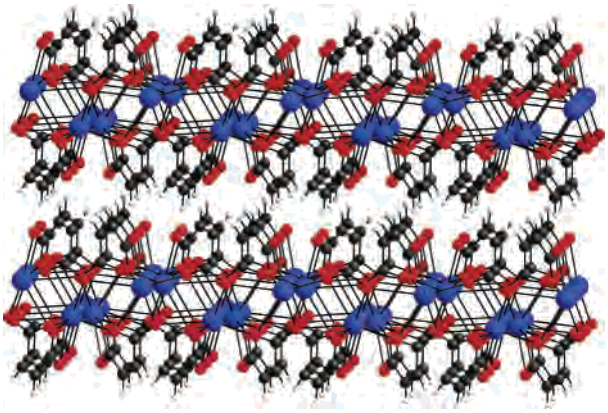

Figure 6. Layered structure of PBMAL, viewed approximately along the *c* axis (black spheres, carbon; red spheres, oxygen; white spheres, hydrogen; blue spheres, lead).

plane (see Figure 6). The single independent lead atom is bonded to seven oxygen atoms (with distances ranging from 2.423(6) to 2.860(8) Å), belonging to four symmetry-equivalent deprotonated maleate ligands (see Figure 7). As in TRIMAL, the coordination sphere around the Pb^{2+} is asymmetric and hemidirected, showing the expression of the lone pair directed along the shortest intralayer Pb−Pb contact of 3.89 Å. Each maleate ligand is bonded to four lead atoms: O1, O3, and O4 are each bonded to two lead atoms, whereas O2 is only bonded to one (see Figure 8). The O2 is situated close to the surface of the layers and participates in two weak hydrogen bonds with H2 and H3 of an adjacent

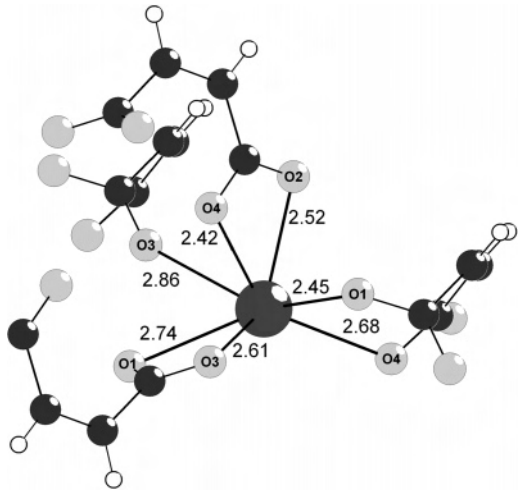

Figure 7. Heptacoordination of Pb by the maleate ligands and relevant distances (Å) in PBMAL.

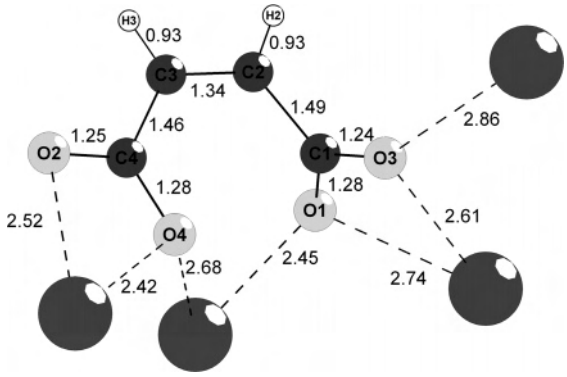

Figure 8. Tetradentate maleate ligand and relevant distances (Å) in PBMAL.

layer at 2.59 and 2.65 Å, respectively. This weak interlayer bonding imparts stability to the overall structure packing. The bond valence sum (BVS)[17,18] for the heptacoordinated lead atom, using a bond cutoff of 2.9 Å, is 1.86, thereby confirming the Pb^{2+} assignment. The four oxygen atoms have a BVS ranging from 1.89 to 1.94, showing that none of the oxygen atoms are protonated. The oxygen O2, which is bonded to only one Pb^{2+} atom, has a BVS of 1.76, which reaches 1.89 when the two hydrogen bonds with H2 and H3 are taken into account. The interlayer volume is too small to accommodate any water molecules.

Thermogravimetric and Elemental Analyses. The thermogravimetric analysis (TGA) of TRIMAL, performed under argon, revealed two distinct thermal events. The first step is ascribed to the gradual loss of the bound lattice water, starting around 50 °C and leading to a plateau in the differential thermal analysis (DTA) signal at 296 °C and a corresponding weight loss of 1.1 wt % (calculated 0.9 wt %). This dehydration step is followed by the decomposition of the compound, giving a sharp loss of 9.5 wt % that peaks in the DTA signal at 358 °C. The decomposition is achieved at about 425°C, and no further thermal events are observed. The final product is PbO, and the corresponding total weight

(17) Brown, I. D.; Altermatt, D. *Acta Crystallogr.* **1985**, *B41*, 244.
(18) Brese, N. E.; O'Keeffe, M. *Acta Crystallogr.* **1991**, *B47*, 192.

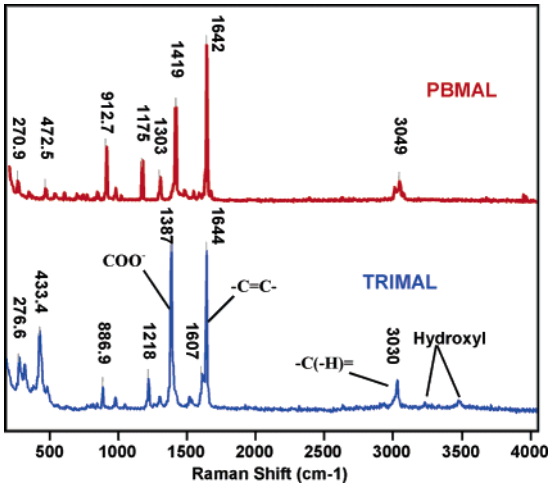

Figure 9. Raman spectra of TRIMAL and PBMAL.

loss is 10.7 wt % at 780 °C, in agreement with the 10.7 wt % calculated for the composition $(Pb_4O_3)[C_2H_2(CO_2)_2]\cdot {}^1/_2H_2O$. One water molecule per formula unit would lead to a calculated loss of 11.5 wt %, whereas an anhydrous phase would lose 9.9 wt %. The elemental analyses are in agreement with the composition derived from the crystal structure. Measured: Pb = 83.9 wt %; C = 4.77 wt %; H = 0.21 wt %. Calculated: Pb = 82.9 wt %; C = 4.80 wt %; H = 0.20 wt %. It should be noted that, whereas water hydrogen cannot be detected by combustion analysis, the hydroxyl hydrogen would be detected. Moreover, no weight loss in the temperature range usually corresponding to the disassociation of a hydroxyl group (400−600 °C) was observed by TGA.

One main weight loss event was noted in the TGA of PBMAL, corresponding to the decomposition of the compound with an onset temperature of 280 °C. No weight loss is observed below 250 °C, confirming the absence of lattice water in the phase. The total weight loss is 30.9 wt %, in agreement with the expected 30.5 wt %. Elemental analyses also confirm the stoichiometry derived from the crystal structure. Measured: Pb = 65.53 wt %; C = 14.83 wt %; H = 0.74 wt %. Calculated: Pb = 64.51 wt %; C = 14.94 wt %; H = 0.62 wt %.

Raman Spectroscopy. The Raman spectra of PBMAL and TRIMAL are given Figure 9. The Raman bands due to distinctive functional groups are labeled: carboxylate (COO^-), alkene (−C═C− and C−H), and hydroxyls. For TRIMAL, there are two Raman bands in the O−H region of the spectrum, peaking near 3229 and 3477 cm^{-1}. Because these two bands have relatively narrow bandwidths, they are probably not hydrogen bonded, i.e., associated with other hydroxyl groups or water molecules. The band peaking near 3229 cm^{-1} is in the region associated with alcohols, but it is significantly narrower than the band commonly observed from alcoholic O−H vibrations. The most likely source of the two O−H bands is water of crystallization in two well-defined crystallographic sites. Both the frequencies of the bands and their narrow bandwidths are consistent with this interpretation. It is of note that the alkene C−H band (3030 cm^{-1}) has a small shoulder on its lower frequency side. The possibility that this feature is due to carboxylic acid groups (−COOH) has been ruled out because, while the frequency is consistent with O−H on carboxylic acid groups, the feature is too narrow. Further, if carboxylic acid groups were present, there would be a more intense band, due to C═O, peaking near 1700 cm^{-1}. This feature is probably an overtone or combination of bands peaking at lower frequency. The Raman spectrum of PBMAL contains essentially the same features as those found in the spectrum of TRIMAL, but some significant differences exist. The spectrum of PBMAL does not include the bands due to hydroxyl species, which we associate with lattice waters in TRIMAL. Other bands, primarily those associated with carboxylate groups (C═O stretch band peaking near 1400 cm^{-1}), are shifted in frequency between the two spectra. These shifts are most likely associated with different structural arrangements of the maleate ligands and their mode of bonding to the lead atoms. To summarize, neither TRIMAL nor PBMAL contain acidic protons (in both cases the maleic acid is deprotonated), and TRIMAL, contrary to PBMAL, does contain water of crystallization.

Table 5. Solid-State NMR Results: Chemical Shifts of the Main ^{13}C and ^1H Resonances

	^{13}C chemical shifts (ppm)		^1H chemical shifts (ppm)	
	carboxylic	olefinic	acid protons	alkene protons
maleic acid	172; 168	139; 132	15.7; 13.0	6.87
TRIMAL	174; 172	136; 131	none	5.91
PBMAL	182; 175	144; 126	none	6.97; 5.65

Solid-State MAS NMR Spectroscopy. A solid-state NMR study has been undertaken to provide further insight into the C and H environments in these compounds as well as additional structure confirmation for TRIMAL. To aid in the interpretation of solid-state NMR data for TRIMAL, maleic acid and PBMAL were also investigated. The chemical shifts of the main ^{13}C and ^1H resonances for the three phases are summarized in Table 5.

Figure 10 shows the ^{13}C CP MAS NMR spectra of maleic acid, TRIMAL, and PBMAL. The spectrum of each compound is comprised of four resonances: two in the carboxylic region and two in the olefinic region. These ^{13}C MAS NMR results reveal that there are several inequivalent carbon environments present within all three compounds. The NMR spectrum of TRIMAL is different from that of maleic acid or PBMAL. The olefinic carbon line widths in TRIMAL are much broader than those observed for maleic acid or PBMAL, indicating an increase in the disorder of the organic species for TRIMAL. In maleic acid, the presence of protons on the carboxylic acid group shifts the observed ^{13}C NMR resonances to about 170 ppm, while the deprotonated carboxylic acid carbons of PBMAL are observed between 175 and 184 ppm. The observed ^{13}C chemical shifts of TRIMAL are intermediate between those of PBMAL and maleic acid, supporting the argument that the TRIMAL carboxylic acids are involved in hydrogen bonding through water instead of acidic protons or direct hydrogen bonding via the methane groups. In addition, the observed splittings of the carboxylic acid and olefinic resonances in TRIMAL

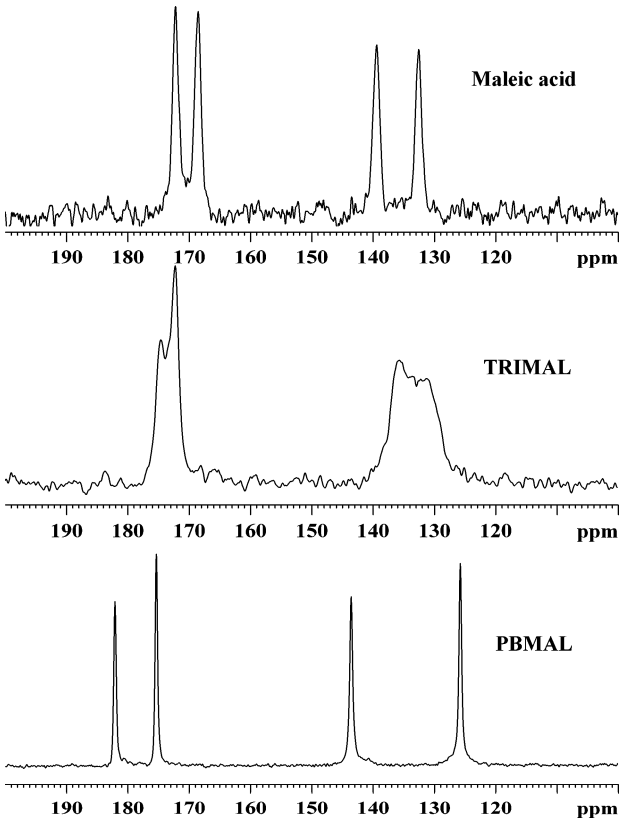

Figure 10. ^{13}C CP MAS NMR spectra.

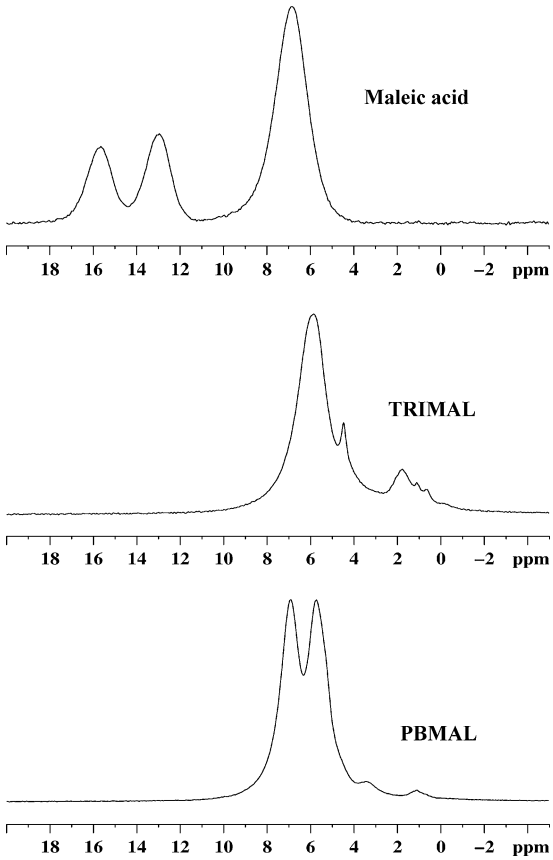

Figure 11. ^{1}H MAS NMR spectra.

(∼2 and 5 ppm, respectively) are smaller than those of maleic acid (∼4 and 7 ppm) or PBMAL (∼7 and 18 ppm). This decrease in chemical shift differences for the carboxylic and olefinic carbons reflects the increased similarity in the local carbon environment from one end of the maleate group to another, consistent with the proposed structure. In fact, our structural model for TRIMAL, described in *C*2/*c*, contains only two independent carbon sites, one olefinic and one carboxylic, with the two sides of the maleate being symmetry related. Although the NMR results (four independent carbon sites) are not fully consistent with this model, the similarity of the chemical shifts for the doublets and the likely presence of disorder of the maleates, evidenced by the line widths of the resonances, show that this more symmetrical model provides, nevertheless, a good description of the compound. When described in *Cc*, a noncentrosymmetric axially polar subgroup of *C*2/*c*, the structural model of TRIMAL does contain four independent carbon sites and is thus consistent with the NMR results. However, the Rietveld refinement using the *Cc* symmetry did not converge, probably because of the high correlation between parameters and the fact that the true distribution of the lead atoms is very close to being centrosymmetric. The positions of the lead atoms refined in *Cc* did converge and are still, within 0.07 Å, related by a center of symmetry. The fact that the majority of the scattering power in the cell possesses pseudosymmetry likely prevents the refinement of the organic part of the structure, which may exhibit a lower symmetry. The large differences in the olefinic carbon ^{13}C NMR chemical shifts in PBMAL reveal that these carbons are inequivalent. This large difference in the local environment is also supported by the distinct alkene proton resonances observed in the ^{1}H MAS NMR spectra (discussed below).

The high-speed ^{1}H MAS NMR spectra (Figure 11) further highlight the deviation of the structure of the organic content in TRIMAL and PBMAL from that of maleic acid. The ^{1}H MAS NMR spectrum of maleic acid shows three resonances at 15.7, 13.0, and 6.87 ppm. The assignment of the two high-frequency resonances to acid protons is consistent with the previously reported literature of 16 and 13.3 ppm.[19] A linear correlation between the ^{1}H NMR chemical shift and the H···O hydrogen bond length in crystals has been given:[20,21] $\delta_{^1H} = 44.68-19.3\ [d_{OH\cdots H}\ (Å)]$, predicting 1.50 and 1.64 Å O···H bond distances for the 15.7 and 13.0 ppm protons, respectively. This leads to the assignment of 15.7 ppm to the intramolecular H bond (O−H =1.59 Å) and of 13 ppm to the intermolecular H bond (O−H = 1.66 Å).[9] The other ^{1}H MAS NMR resonance for maleic acid at 6.87 ppm is assigned to the alkene protons. This assignment is consistent with 6.2 ppm observed for the alkene protons of maleic acid dissolved in $CDCl_3$. The lack of any resonances at >8 ppm in either TRIMAL or PBMAL clearly demonstrates that there are no acidic protons present within these phases, consistent with the nonprotonated carboxylic acid obtained through structure refinement and with the chemical analysis results.

(19) Harris, R. K.; Jackson, P.; Merwin, L. H.; Say, B. J.; Hagele, G. *J. Chem. Soc., Faraday Trans.* **1988**, *84*, 3649.
(20) Jeffery, A.; Yeon, Y. *Acta Crystallogr., Sect. B* **1986**, *42*, 410.
(21) Alam, T. M.; Fan, H. *Macromol. Chem. Phys.* **2003**, *204*, 2023.

This is also consistent with the lack of carboxylic acid stretches in their Raman spectra.

The ^{1}H MAS NMR spectrum of TRIMAL is dominated (78%) by the single resonance at 5.91 ppm, which is assigned to the olefinic protons in this sample. There are also numerous resonances between 4.5 and 0.7 ppm, which are assigned to either OH or H_2O proton species. This range of chemical shifts supports the idea that we have different types of water environments present within the material. The observation of only a single resonance for the two alkene protons indicates that they have chemically similar environments. On the other hand, the ^{1}H MAS NMR spectrum of PBMAL shows two nonequivalent alkene proton resonances at 6.97 and 5.65 ppm (each 47.5%). This large inequivalency is consistent with the large splitting of the alkene resonance observed in the ^{13}C CP MAS spectrum of this compound. Also observed are two minor resonances at 3.3 and 1.02 ppm that can be assigned to either H_2O or OH. These species constitute only 5% of the total ^{1}H density. Heating at 100 °C did not reduce or change the intensity of these signals that could originate from a minor amorphous impurity not detected by X-ray diffraction.

To investigate spatial relationships and to further support the assignment of the different hydrogen environments in these materials, 2D DQ correlation NMR spectra were obtained. Figure 12 shows the 2D DQ NMR spectra for maleic acid, TRIMAL, and PBMAL. These types of ^{1}H DQ MAS NMR exchange experiments consist of a single-quantum dimension (horizontal) plotted versus the DQ dimension (vertical). The observation of correlations, or cross-peaks, arises because of the dipolar coupling between different protons. For the mixing times used in the present DQ exchange experiments, the presence of a correlation implies that the dipolar-coupled protons are separated by $<$5Å. The lack of a DQ correlation may be the result of too long ^{1}H$-^1$H distances (weak dipolar couplings) or a reduction (averaging) of the dipolar coupling due to molecular motions. Resonances that occur along the diagonal (ω, 2ω) are referred to as autocorrelation peaks and result from dipolar interactions between protons with the same chemical shift. Off-diagonal resonances (ω_a, $\omega_a + \omega_b$) and (ω_b, $\omega_b + \omega_a$) are produced by dipolar interactions with different chemical shifts.

The ^{1}H DQ MAS NMR exchange spectrum for maleic acid (Figure 12a) shows many different correlation resonances. The acidic protons at 15.7 and 13.0 ppm show a strong correlation in between (resonance AB), revealing that there are close intermolecular contacts between the acid protons of the carboxylic groups. The lack of or small intensity of autocorrelation peaks for the acid resonances (AA and BB) reveals that protons of similar environments are not spatially near each other in the material; they are actually more than 4 Å apart. The acid protons also show correlations with the olefinic protons (AC and BC) again consistent with the spatial closeness in the maleate group ($d = 2.70$ Å). The unresolved methane protons show a strong autocorrelation peak (CC) also consistent with the proposed structure where the methane protons are 2.24 Å apart. A weak autocorrelation

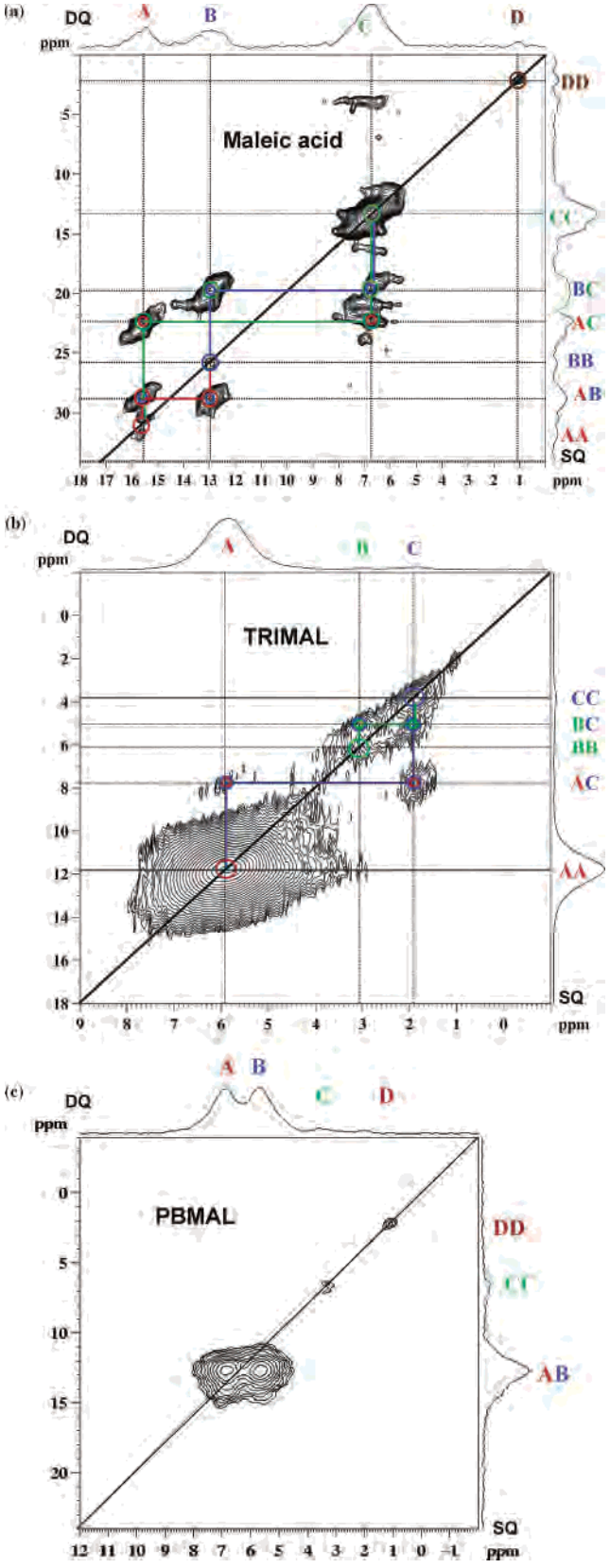

Figure 12. 2D ^{1}H DQ MAS NMR spectra of (a) maleic acid, (b) TRIMAL, and (c) PBMAL.

peak is observed at ~1 ppm (DD), resulting from trace water within the maleic acid structure. The ^{1}H DQ MAS spectrum for TRIMAL (Figure 12b) is different in appearance. In this

spectrum, the dominant peak is the autocorrelation resonance (AA) for the nonresolved methane protons. There are also a series of autocorrelation resonances (BB and CC) for the different water species, as well as spatial correlation between these two different water species (BC). Finally, there is a weak but significant correlation between the water resonance at 1.9 ppm and the methane resonance at 5.9 ppm, revealing that in TRIMAL there are water species spatially near the olefinic protons of the maleate group. The 2D ^{1}H DQ MAS NMR spectrum of PBMAL (Figure 12c) clearly shows the correlation between the resolved nonequivalent olefinic protons of the maleate group (AB), with no autocorrelation peaks (AA or BB) observed. This is consistent with the short ^{1}H$-^1$H distance of 2.21 Å being the intramolecular connectivity of these protons. Weak autocorrelation peaks between the residual water resonances (CC and DD) were also observed, but no correlations between the alkene protons and the residual water were observed. This confirms that water is not spatially located near the maleate group in PBMAL, consistent with the lack of water of crystallization found by the structural analysis and TGA measurement. It is likely that this small amount of residual water belongs to a minor impurity phase not detected by X-ray powder diffraction or to surface-adsorbed water.

Conclusions

We have determined from X-ray powder diffraction the structure of tribasic lead maleate (TRIMAL) and confirmed the adequacy of the derived structural model using Raman spectroscopy and ^{1}H MAS and ^{1}H$-^{13}$C CP MAS NMR experiments. TRIMAL consists of infinite one-dimensional slabs of composition [Pb_4O_3], linked together into a three-dimensional network by tetradentate deprotonated maleate ligands. We have also synthesized and characterized a related phase, lead maleate (PBMAL), which provided a reference point for the interpretation of the spectroscopic data collected on the tribasic compound. The Raman and NMR data confirmed that the maleate ligands are deprotonated in both TRIMAL and PBMAL and that the structure of TRIMAL contains water of crystallization. The structure determination of TRIMAL represents a first step toward the understanding of the structure−property relationships of basic lead carboxylates and thus the optimization of their performance as thermal stabilizers of halogenated polymers.

Acknowledgment. This research was supported by Sandia National Laboratories' Laboratory-Directed Research and Development program (Grant DE-FG07-1ER63282). Sandia National Laboratories is a multiprogram laboratory operated by Sandia Corp., a Lockheed Martin Co. for the U.S. Department of Energy's National Nuclear Security Administration under Contract DE-AC04-94AL85000. The authors thank Dr. Dick Grossman, formerly with Halstab, for his comments and help on the TRIMAL synthesis. J.B.P. and A.J.C. acknowledge the Center for Environmental and Molecular Sciences NSF-CHE-0221934 and NSF-DMR-0452444.

Supporting Information Available: X-ray crystallographic data for TRIMAL and PBMAL, in CIF format. This material is available free of charge via the Internet at http://pubs.acs.org.

IC050611Y